Dynamics of Disk and Elliptical Galaxies in Refracted Gravity

Valentina Cesare[1,2], Antonaldo Diaferio[2,3], Titos Matsakos[2], Garry Angus[2]

[1] INAF, Osservatorio Astrofisico di Catania, via Santa Sofia 78, 95123 Catania, CT, Italia

[2] Dipartimento di Fisica, Università di Torino, via Pietro Giuria 1, 10125 Torino, TO, Italia

[3] Istituto Nazionale di Fisica Nucleare (INFN), Sezione di Torino, Torino, Italia

Abstract

We test Refracted Gravity (RG) [1] by investigating the dynamics of disk galaxies in the Disk Mass Survey (DMS) [2,3,4] and of three elliptical E0 galaxies in the SLUGGS survey [3,4,5] without the aid of dark matter. RG reproduces the rotation curves, the vertical velocity dispersions, and the observed Radial Acceleration Relation (RAR) of DMS galaxies and the root-mean-square (RMS) velocity dispersions of stars, and blue and red globular clusters in the E0 galaxies. Our results show that RG can compete with other theories of gravity to describe the gravitational dynamics on galaxy scale.

1. INTRODUCTION

In Newtonian gravity, we can model the observed rotation curves in the external regions of disk galaxies by assuming the presence of dark matter. This mass discrepancy can be neatly quantified by the RAR [6], which shows that the observed radial acceleration traced by the rotation curves ($g_{\rm obs}$) is tightly correlated with the Newtonian acceleration due to the baryonic matter distribution ($g_{\rm bar}$). The observed RAR is fitted by this relation [6]:

$$g_{\rm obs}(R) = \frac{g_{\rm bar}(R)}{1-\exp\left(-\sqrt{g_{\rm bar}(R)/g_\dagger}\right)}, \qquad (1)$$

where $g_\dagger = (1.20 \pm 0.02 \pm 0.24) \times 10^{-10}\ {\rm m/s^2}$ is consistent with the MOND acceleration scale $a_0 = 1.20 \times 10^{-10}\ {\rm m/s^2}$.

Newtonian gravity needs dark matter also to reproduce the velocity dispersions in the outermost regions of elliptical galaxies, probed by the detection of kinematic tracers, such as globular clusters (GCs) or planetary nebulae. Specifically, the mass discrepancy in these systems might be positively correlated with their ellipticity [7].

2. REFRACTED GRAVITY

Refracted Gravity (RG) [1] is a classic theory of gravity whose field equations yield the modified Poisson equation:

$$\nabla \cdot [\epsilon(\rho)\nabla\phi] = 4\pi G\rho, \qquad (2)$$

where the permittivity $\epsilon(\rho)$ is an arbitrary monotonic function of the mass density ρ with the asymptotic limits $\epsilon(\rho)=1$ for $\rho \gg \boldsymbol{\rho_c}$ and $\epsilon(\rho) = \boldsymbol{\epsilon_0}$ for $\rho \ll \boldsymbol{\rho_c}$. As a test case, we adopt the function

$$\epsilon(\rho) = \boldsymbol{\epsilon_0} + (1-\boldsymbol{\epsilon_0})\frac{1}{2}\left\{\tanh\left[\ln\left(\frac{\rho}{\boldsymbol{\rho_c}}\right)^{\boldsymbol{Q}}\right]+1\right\}, \qquad (3)$$

with $\boldsymbol{\epsilon_0}$, $\boldsymbol{Q}$, and $\boldsymbol{\rho_c}$ free universal parameters (Fig. 1). Figure 2 compares the gravitational fields in Newtonian and Refracted gravities, for flat and spherical systems. In RG, the acceleration boost in flat systems is due to the focusing of force lines rather than to the presence of dark matter as in Newtonian gravity.

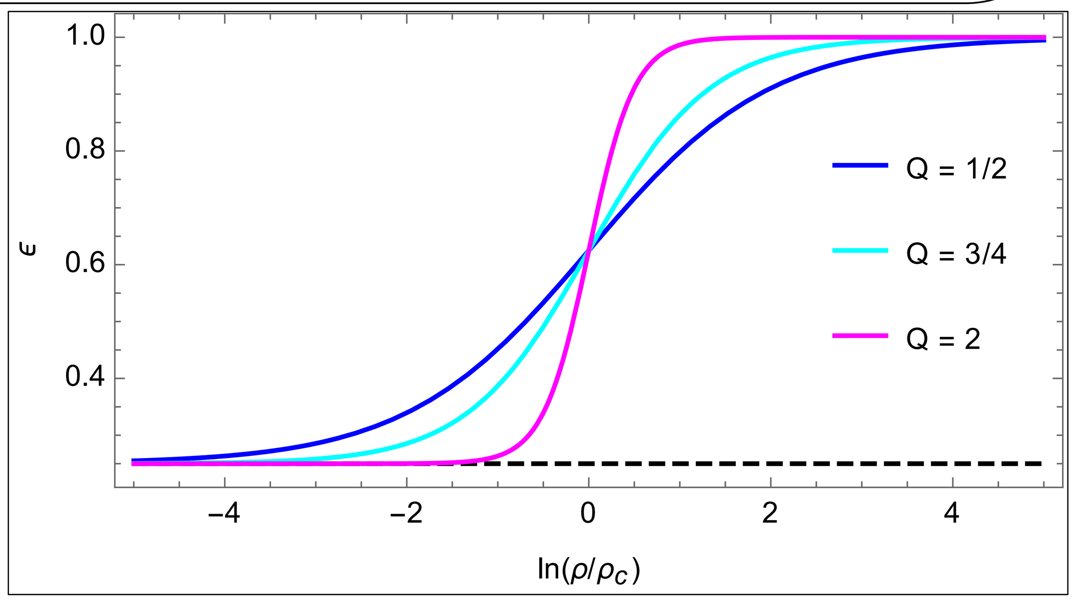

Figure 1

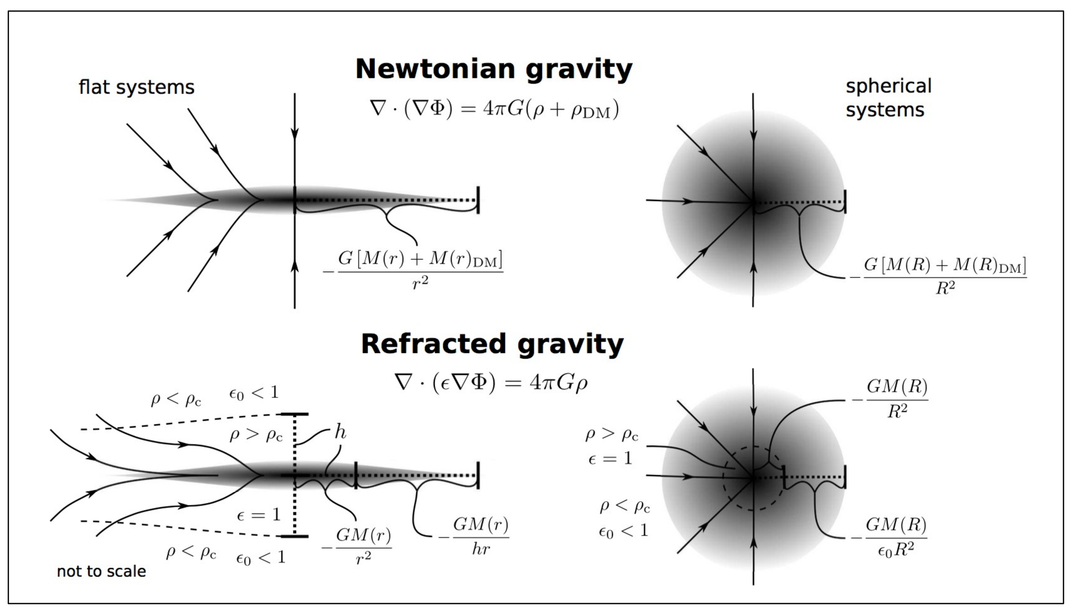

Figure 2

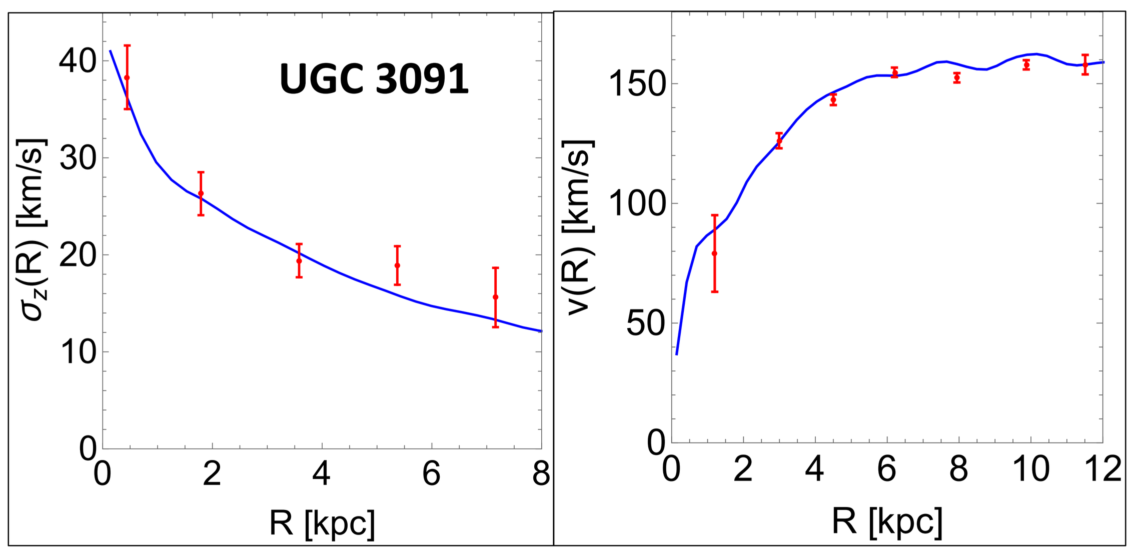

Figure 3

3. ROTATION CURVES AND VERTICAL VELOCITY DISPERSIONS OF DISK GALAXIES

We consider 30 disk galaxies from the DMS [8]. We model the mass distribution with **(1) a stellar disk**, **(2) a spherical stellar bulge**, and **(3) an atomic and molecular gas components**.

We solve the RG Poisson equation (Eq. (2)) with a Successive Over Relaxation numerical method and use a MCMC algorithm to estimate the mass-to-light ratio, $\boldsymbol{\Upsilon}$, the disk scale height, $\boldsymbol{h_z}$, and the 3 RG parameters, $\boldsymbol{\epsilon_0}$, $\boldsymbol{Q}$, and $\boldsymbol{\rho_c}$, from the two kinematic profiles at the same time. Figure 3 shows one example. Both profiles are well described with **sensible $\boldsymbol{\Upsilon}$ and $\boldsymbol{h_z}$** and with **RG parameters consistent among different galaxies, suggesting their universality** (Fig. 5). The flat trend in the outer region of the rotation curve is properly reproduced by RG.

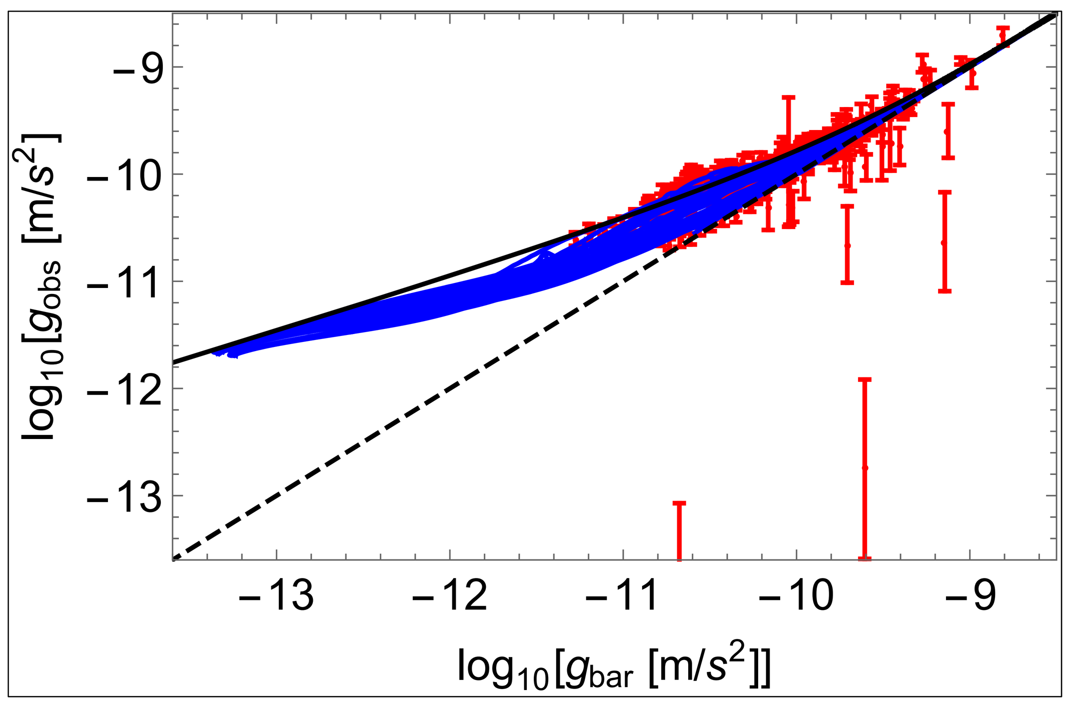

Figure 4

4. RAR IN DMS

Figure 4 shows the RAR for DMS galaxies. The points with error bars show the data of the DMS sample, the black curve is Eq. (1), and the blue lines are the RG models, derived with the parameters found in point 3. $g_{\rm obs}$ is the centripetal acceleration $\frac{v_{\rm obs}^2}{R}$ implied by the observed rotation curve $v_{\rm obs}(R)$ and $g_{\rm bar}$ is the baryonic radial acceleration, $\frac{\partial\phi_{\rm N}}{\partial R}$, obtained by solving the Newtonian Poisson equation, $\nabla^2\phi_{\rm N} = 4\pi G\rho$, where ρ is the sum of the contributions **(1)**, **(2)** and **(3)**. **The two asymptotic limits for large and small $g_{\rm bar}$ of Eq. (1) are properly reproduced by RG.**

5. RMS VELOCITY DISPERSIONS OF E0 GALAXIES

We consider 3 E0 galaxies from the SLUGGS survey [9]. We model, at the same time, the RMS velocity dispersions of the 3 kinematic tracers, **stars**, **blue GCs**, and **red GCs**, with spherical Jeans analysis:

$$V_{\rm rms,t}^2(R) = \frac{2G}{I_{\rm t}(R)}\int_R^{+\infty} K\left(\boldsymbol{\beta_{\rm t}}, \frac{r}{R}\right)\nu_{\rm t}(r)\frac{M(r)}{\epsilon(\rho)}\frac{{\rm d}r}{r}, \qquad (4)$$

where $M(r)$ is the mass profile, which includes **(1) stars**, **(2) gas**, and **(3) central SMBH**, and $I_{\rm t}(R)$, $\nu_{\rm t}(r)$, and $\boldsymbol{\beta_{\rm t}}$ are the surface brightness/number density, the 3D luminosity/number density, and the orbital anisotropy parameter of each tracer t. We estimate the mass-to-light ratio, $\boldsymbol{\Upsilon}$, the 3 RG parameters and the 3 $\boldsymbol{\beta_{\rm t}}$ from the data with a MCMC. Figure 6 shows the result for NGC 1407: RG properly describes the dynamics of the three populations with **a unique set of RG parameters consistent, at most within 3σ, with the one retrieved from the other two E0 galaxies and from the DMS galaxies (Fig. 5).**

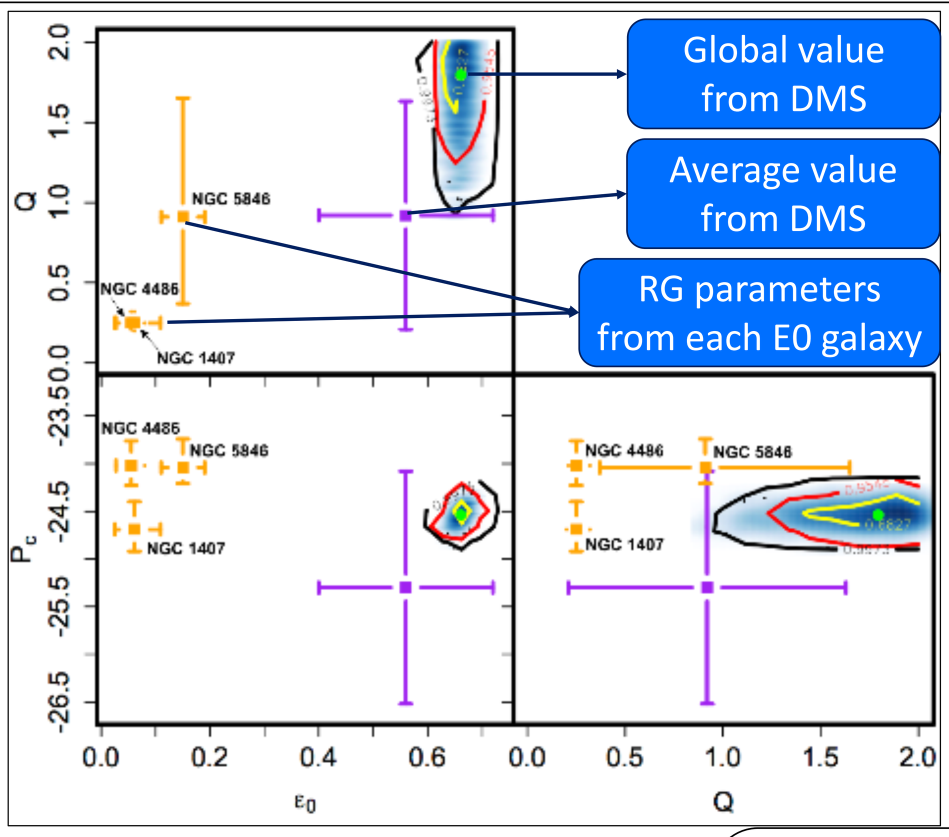

Figure 5

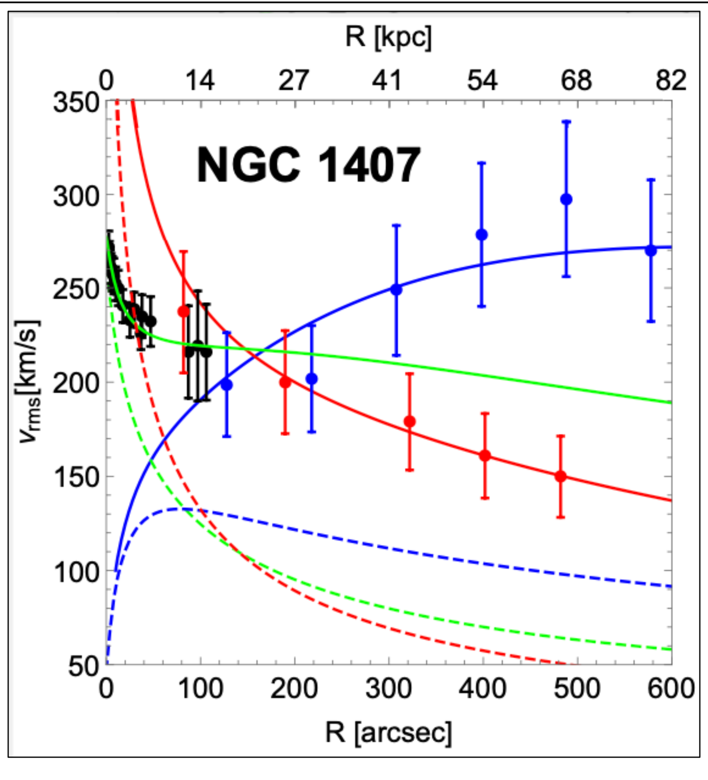

Figure 6

References

[1] Matsakos, T., & Diaferio, A., 2016, ArXiv e-prints [arXiv:1603.04943]
[2] Cesare, V., Diaferio, A., Matsakos, T., & Angus, G., 2020, A&A, 637, A70
[3] Cesare V., 2021, Phys. Sci. Forum, 2(1), 34
[4] Cesare V., 2023, Universe, 9(1), 56
[5] Cesare V., Diaferio, A., & Matsakos, T., 2022, A&A, 657, A133
[6] McGaugh, S. S., Lelli, F., & Schombert, J. M., 2016, Phys. Rev. Lett., 117, 201101
[7] Deur, A., 2014, MNRAS, 438, 1535
[8] Bershady, M. A., Verheijen, M. A. W., Swaters, R. A., et al., 2010a, ApJ, 716, 198
[9] Forbes, D. A., Alabi, A., Brodie, J. P., et al., 2017, AJ, 153, 114